[CANCER RESEARCH 62, 4773–4780, August 15, 2002]

FOXM1 Is a Downstream Target of Gli1 in Basal Cell Carcinomas[1]

Muy-Teck Teh,[2,3] Soon-Tee Wong,[2,4] Graham W. Neill, Lucy R. Ghali, Michael P. Philpott, and Anthony G. Quinn

Centre for Cutaneous Research, Barts & The London School of Medicine and Dentistry, Queen Mary, University of London, London E1 2AT, United Kingdom

ABSTRACT

Forkhead box (FOX) proteins have been shown to play important roles in regulating the expression of genes involved in cell growth, proliferation, differentiation, longevity, and transformation. The functional importance of this gene family in normal human skin physiology and disease processes is not well understood. Activation of Sonic Hedgehog (Shh) signaling plays a key role in the development of basal cell carcinomas (BCCs) of the skin in humans. Recent studies have established that some *FOX* genes are downstream targets of Shh signaling. We have investigated the role of FOX proteins in transducing Shh effects in human skin by using degenerate PCR to identify FOX genes differentially expressed in BCCs. All three known FOXM1 isoforms (a, b, and c) were detected in human skin and cultured keratinocytes, and the transcriptionally active FOXM1b isoform was found to be up-regulated in BCCs. Real-time quantitative RT-PCR showed that the increase in FOXM1 mRNA levels was specific for BCCs and not a reflection of increased cell proliferation in that no up-regulation was seen in squamous cell carcinomas or proliferating primary human keratinocyte cultures. Immunostaining studies showed intense nuclear and cytoplasmic staining throughout BCC tumor islands and not confined to the periphery regions of the tumor where proliferating Ki-67-immunopositive cells are predominantly localized. Expression of the Shh target glioma transcription factor-1 (Gli1) in primary keratinocytes and other cell lines caused a significant elevation of FOXM1 mRNA level and transcriptional activity, indicating that FOXM1 is a downstream target of Gli1. Our data provide the first evidence that activation of Shh signaling via Gli1 is an important determinant of FOXM1 expression in mammalian cells. Given the role of FOXM1 in cell proliferation, the up-regulation of FOXM1 in BCCs may be one of the mechanisms whereby Shh signaling exerts its mitogenic effect on basal keratinocytes, leading to the development of this common human cancer.

INTRODUCTION

Winged-helix/FOX[5] proteins, which constitute a large family of transcription factors, have been implicated in both embryonic development and adult tissue homeostasis by regulating cell growth, proliferation, differentiation, longevity, and transformation (reviewed in Ref. 1). Recently, all known winged-helix/forkhead members have been assigned a unified nomenclature—the FOX family (2). FOX proteins are defined by a conserved DNA-binding protein motif (WD) of ~100 amino acids, which was first identified in HNF-3γ/*Foxa3* (3, 4).

Hedgehog signaling is important in the regulation of patterning, cell cycle and proliferation, survival, and growth of embryos and various adult tissues. Inappropriate maintenance of hedgehog signaling pathway has been implicated in various tumor development in the skin, muscle, and brain (reviewed in Refs. 5 and 6). There are three known members of the hedgehog-secreted glycoprotein family in mammals, namely Sonic, Desert, and Indian hedgehog. Shh has been shown to be the most potent (7) and most widely expressed in both embryos and adult tissues (reviewed in Ref. 8). The zinc-finger Gli1 is one of the key downstream targets of Shh signaling via a membrane-receptor complex composed of PTCH1 and SMO, and a complex cascade of intracellular mediators (6). Physiologically, activation of Shh signaling is initiated by the binding of the Shh protein to PTCH1 receptor, which in turn releases its inhibition on SMO, resulting in the activation of Gli. Inappropriate expression of Gli1 has been shown to be a crucial event in tumorigenesis of the brain and skin (5).

In previous work, we and others have established that activation of Shh signaling, by mutational inactivation of the Shh receptor PTCH1 (9), activating mutation of the PTCH1-binding G-protein-coupled receptor SMO (10), or up-regulation of a Shh target transcription factor Gli1 (11–14), plays a key role in the development of the common Caucasian skin cancer, BCC. Moreover, a number of murine FOX genes, such as the induction of *Foxa2* (HNF-3β) during floor plate development (15), *Foxd2* (Mf-2) during somitogenesis (16), and *Foxf1* (FREAC-1 or HFH-8) during lung and foregut organogenesis (17), have been shown to be expressed within areas of active Shh signaling. The authors have established that these *FOX* genes are direct targets of Shh during embryonic development of the mice.

In view of the role of some *FOX* genes in mediating Shh signaling, we have investigated the expression of this gene family in normal human skin, primary cultured human keratinocytes, and BCC and SCC samples. Using degenerate PCR and real-time PCR, we have found that FOXM1 (previously known as HFH-11, INS-1, WIN, MPP2/MPHOSPH2, or Trident/FKHL16) is specifically up-regulated in BCCs but not in normal skin, cultured keratinocytes, or SCCs. Previous studies have shown that FOXM1 has a wide cellular pattern of expression in various mescenchymal and epithelial cells during embryonic development (18), whereas in adult mice FOXM1 expression was confined to the thymus, intestine, colon, and testis (18–21). Although studies have shown that FOXM1 expression in murine hepatocytes was activated in response to mitogens, hepatectomy (22), or toxin-induced liver damage (23), FOXM1 expression has not been previously linked to Shh signaling. Little is known about FOXM1 expression in human skin and its implication in tumor formation. In the present study, we present the first evidence that the increased expression and activity of FOXM1 in BCCs, characterized by activated Shh signaling, is a downstream target of the Shh effector Gli1 transcription factor.

MATERIALS AND METHODS

Oligonucleotides. The oligonucleotides used were: FkhDF, 5′-CGC*AAGCT*-*T*AARCCHCCHTAWTCNTAYAT-3′ and FkhDR, 5′-GCG*GTCGAC*RTGYCKRATNGARTTCTGCCA-3′; GapF, 5′-C_{292}CCATCACCATCTTCCAGGA-GC_{313}-3′ and GapR, 5′-C_{764}CAGTGAGCTTCCCGTTCAGC_{744}-3′ (based on the human GAPDH; GenBank accession no. NM_002046); βActinF, 5′-G_{442}TTTGAGACCTTCAACACCCC$_{462}$-3′ and βActinR, 5′-G_{759}TGG-CCATCTCTTGCTCGAAGTC$_{737}$-3′ (human β-actin; GenBank accession no.

Received 3/18/02; accepted 6/20/02.

The costs of publication of this article were defrayed in part by the payment of page charges. This article must therefore be hereby marked *advertisement* in accordance with 18 U.S.C. Section 1734 solely to indicate this fact.

[1] Supported by the Wellcome Trust Grant (to M-T. T. and A. G. Q.), the Cancer Research UK (to A. G. Q.), and the Medical Research Council (to G. W. N. and A. G. Q.).

[2] These authors contributed equally to this work.

[3] To whom requests for reprints should be addressed, at Centre for Cutaneous Research, Barts & The London School of Medicine and Dentistry, Queen Mary, University of London, 2 Newark Street, Whitechapel, London E1 2AT, United Kingdom. Phone: 44-207-882-7170; Fax: 44-207-882-7171; E-mail: m.t.teh@qmul.ac.uk.

[4] Present address: Division of Dermatology, Department of Medicine, National University of Singapore, 5 Lower Kent Ridge Road, Singapore 119074.

[5] The abbreviations used are: FOX, forkhead box; BCC, basal cell carcinoma; SCC, squamous cell carcinoma; EGFP, enhanced green fluorescence protein; Shh, sonic hedgehog; Gli1, glioma transcription factor 1; AP, alkaline phosphatase; WD, winged-helix DNA-binding domain; GAPDH, glyceraldehyde-3-phosphate dehydrogenase; HNF, hepatocyte nuclear factor; SMO, smoothened; PTCH1, patched-1; SIN-IP-GFP, *S*elf-*In*activating-*I*nternal *P*romoter-*G*reen *F*luorescence *P*rotein.

XM_037235); FoxF1, 5′-GCG*AAGCTT* A_{108}TGAAAACTAGCCCCCGT$_{125}$-3′ and FoxR1, 5′-GCG*GAATTC*C_{2354}TACTGTAGCTCAGGAAT$_{2337}$-3′; FoxF2, 5′-GCGACT*CTCGAG*CATG$_{728}$GAGAATTGTCACCTG$_{743}$-3′ and FoxR2, 5′-GCGCTA*CTCGAG* T_{1136}TCGGTTTTGATGGT$_{1122}$-3′; FoxF3, 5′-G_{1145}GGC-GCACGGCGGAAGATGAA$_{1165}$-3′ and FoxR3, 5′-C_{1523}CACTCTTCCAAG-GGAGGGCTC$_{1502}$-3′. All three pairs of Fox primers were designed based on HFH11b mRNA (U74613). FoxF2 and R2 primers encompass the WD and the alternatively expressed A1 exon, whereas FoxF3 and R3 primers encompass A2 exon (see Fig. 2*B*). GliF, 5′-GCG*GAGCTC*A_{79}TGTTCAACTCGATG A_{94}-3′ and GliR, 5′-GCG*AAGCTT*G_{3396}GCACTAGAGTTGAG$_{3382}$-3′; 5BS-F, 5′-*CTAG*C-(TACGTTGTTAT TTGTTTTTTTCG)$_5$C-3′ and 5BS-R, 5′-*TCGAG*(CGAAAA-AAACAAATAACAACGTA)$_5$G-3′.

Degenerate PCR and Northern Analysis. On the basis of previous study (24, 25), the pair of degenerate primers FkhDF and FkhDR were designed to amplify a PCR product containing the consensus KPPYSYI and WQNSIRH amino acid sequences within the highly conserved WD. cDNA samples from polled normal skin ($n = 7$), and BCCs ($n = 7$) were used as templates for the degenerate PCR (Stragene Robocyler; Stragene, La Jolla, CA) under the following cycling profile: initial denaturation (2 min, 94°C), followed by 40 cycles of 45 s at 94°C, annealing for 2 min at 51°C and elongation for 1 min at 68°C, and terminated by a final elongation period at 68°C for 10 min. Gel-purified and *Hind*III-*Sal*I-digested PCR fragments were subcloned into pGEM1 plasmid (Promega, Madison, WI). Clones were sequenced (BigDye™ Terminator Cycle Sequencing Kit; Applied Biosystems, Foster City, CA) and identified by using the NCBI BLAST (http://www.ncbi.nlm.nih.gov/BLAST/) sequence alignment analysis against the nucleotide databases. Putative FOXM1-positive clones were further confirmed by sequencing analysis on nonwinged-helix regions of the gene and Southern dot-blot hybridization (data not shown). Northern analysis was performed as described previously (26). Briefly, the cDNA probe for Northern hybridization of FOXM1 was generated by PCR amplification (using FoxF1 and FoxR1 primers) from a FOXM1b (HFH11b; Ref. 18) clone kindly provided by Dr. Robert Costa (University of Illinois at Chicago, Chicago, IL). The cDNA probe for human β-actin was PCR amplified using βActinF and βActinR primers from a normal human skin genomic DNA. Gel-purified PCR products were subsequently labeled with α-^{32}P dCTP (Amersham Pharmacia Biotech, Little Chalfont, United Kingdom) using the Megaprime™ DNA labeling system (Amersham). Poly-A^+ mRNA extracted from samples (as described in Ref. 26) was size-fractionated by agarose gel-electrophoresis under formaldehyde (~6%) denaturing condition and mRNA transferred onto hybridization membranes (Hybond-XL; Amersham). Membranes were hybridized (overnight at 42°C) with the ^{32}P-labeled probes. After a series of buffer washes, the membranes were exposed to a Phosphor Screen and hybridization signals were detected using a Phosphorimager (Molecular Dynamics, Sunnyvale, CA).

RT-PCR. Poly-A^+ mRNA was extracted directly from tissues or cells in culture using the Dynabeads® mRNA Direct™ kit (Dynal ASA, Oslo, Norway), and purified mRNA was then reverse transcribed into cDNA using the Reverse Transcription System kit (Promega). Control untranscribed mRNA was used as a control for genomic DNA contamination in subsequent PCR analysis. None of these mRNA controls produced any PCR products eliminating genomic DNA contamination as a confounding artifact. Furthermore, all primers used in this study were designed to amplify products with exons encompassing multiple introns, hence any genomic DNA contamination in PCR would give rise to significantly larger sized products. Such contamination has not occurred in the present study.

Real-Time Quantitative PCR. For quantification of FOXM1 mRNA transcripts, the pair of primers FoxF2 and FoxR2 were used to PCR amplify (Hybaid MultiBlock System) the WD (~436 bp) of FOXM1 from a pooled cDNA sample of primary human keratinocyte. The PCR product was purified after gel electrophoresis and quantified densitometrically (Easy Plus Imaging System; UVP Ltd., Cambridge, United Kingdom) using standard DNA quantification ladders. A serial dilution of this template FOXM1 cDNA was used to generate a standard curve comprising 0.01–1000 fg (equivalent to a range of 21 to 2.1×10^6 copies of FOXM1 mRNA) using the LightCycler (see below). The mRNA copy number of FOXM1 in each sample was determined from the standard curve using the LightCycler quantification software as described previously (27). The human GAPDH was used as a reference housekeeping gene for all quantification of FOXM1 mRNA levels. The GapF and GapR primers were used to PCR amplify a fragment (473 bp) of GAPDH from a cDNA sample of primary human keratinocyte. Similarly, a standard titration curve for GAPDH was performed, and the mRNA copy number of GAPDH in each sample was determined as described above. The amount of FOXM1 mRNA in each sample was normalized against the amount of GAPDH mRNA in the same sample and subsequently expressed as the mRNA copy number of FOXM1 per 1000 copies of GAPDH mRNA.

Real-time quantitative PCR was performed using a LightCycler™ rapid thermal cycler instrument (Roche Diagnostics Ltd., Lewes, United Kingdom) in which PCR reactions were performed in a 10-μl volume, in the LightCycler glass capillaries, containing 0.5 μM primers and $MgCl_2$ concentration optimized for each pair of primers between 2 and 5 mM. *Taq* DNA polymerase, DNA double-strand specific SYBR Green I dye, nucleotides, and buffer were included in the FastStart DNA Master SYBR Green I mix (Roche Diagnostics Ltd.). A typical protocol comprised an initial denaturation at 95°C for 10 min, followed by 40 cycles of 95°C for 15 s, 60(FOXM1)/55(GAPDH)°C annealing for 10 s, and 72°C elongation for 17–19 s (depending on the length of the product, 1 s/25 bp). Fluorescence was measured at 2~3°C below specific melting peak of each product (see below; *i.e.*, 84°C for FOXM1 and 86°C for GAPDH) when the respective DNA products were double stranded at these temperatures. At the end of the 40 cycles, samples were subjected to a melting analysis to confirm amplification specificity of the PCR products. During this step, samples were heated from 65–95°C at a steady rate of 0.1°C/s, and fluorescence was measured continuously throughout this period. Melting analysis of FOXM1 and GAPDH of all cDNA samples amplified, consistently (both intra- and inter-experiment) gave single melting peaks of 86.96 ± 0.10°C (mean ± SE of $n = 12$, randomly chosen samples from three independent experiments) and 88.21 ± 0.05°C, respectively. PCR products were further confirmed by gel electrophoresis.

Immunohistochemistry and Fluorescence Microscopy. FOXM1 was immunostained with a previously characterized rabbit polyclonal antibody (18) kindly provided by Dr. Robert Costa. Proliferating cells were immunostained with Ki-67 rabbit polyclonal antibody purchased from DAKO Ltd. (Cambridgeshire, United Kingdom). Gli-1 was immunostained with a goat polyclonal antibody Gli-1 (C-18, sc-6152; Santa Cruz Biotechnology, Santa Cruz, CA) as described previously (12). Paraffin sections were immunostained as described (12). Reaction product was visualized using diaminobenzidine as a chromogenic substrate. Cultured cells expressing EGFP were visualized using a light microscope (Leica DM IRB) fitted with a Krypton/Argon mixed-gas laser for emitting excitation wavelength at 488 nm. Images were captured with a digital imaging system (Leica DC200 imager with a DC Viewer software V3.2; Leica Microsystems Ltd., Heerbrugg, Germany) attached to the microscope. Digitized fluorescence images were subsequently annotated using the software Corel Draw/Photo-Paint V10 (Corel Corporation Ltd., Ontario, Canada).

Plasmids Construction. A coding sequence of the human FOXM1b (nucleotides 108-2354, amino acids 1–748, U74163) was PCR amplified (MultiBlock System; Hybaid Ltd., Ashford, Middlesex, United Kingdom) using FoxF1 and FoxR1 primers from a FOXM1b (HFH11b) clone (18). The purified PCR product was digested (*Hind*III-*Eco*RI) and inserted into plasmid pEGFP-C3 (Clontech) to generate a fusion construct, pEGFP-FOXM1b, which was later subcloned into a retroviral SIN-IP-GFP vector (28). SIN-IP-GFP was digested with *Xho*I-*Eco*RI to remove the IP-GFP sequence and subsequently ligated with the *Sal*I-*Eco*RI digested CMV-EGFP-FOXM1b fragment (from a modified version of pEGFP-FOXM1b with an adapter containing additional restriction site *Sal*I inserted into an *Ase*I site upstream of CMV) to produce the plasmid SIN-EGFP-FOXM1b. Gli1 coding cDNA (a kind gift from Dr. Kenneth Kinzler, Johns Hopkins Medical Institutions, Baltimore, MD; Ref. 29) was amplified by PCR with the GliF and GliR primers. The Gel-purified product was then digested (*Sac*I-*Hind*III) and inserted into pEGFP-C3 to generate a fusion construct pEGFP-Gli1. SIN-EGFP-Gli1 was generated using an identical approach described for FOXM1b. All plasmid constructs described were verified by restriction enzyme digestion and sequencing analyses (BigDye™ Terminator Cycle Sequencing Kit; Applied Biosystems).

A specific FOXM1-binding nucleotide sequence has been characterized previously (no. 24 binding site; Ref. 18). The pair of complimentary oligonucleotides 5BS-F and 5BS-R were synthesized to create a sequence containing five consecutive repeats of the no. 24 FOXM1 binding site (5BS) flanked with sticky *Nhe*I-*Xho*I ends. The pair of oligonucleotides were annealed in a buffer (75 mM NaCl, 5 mM Tris-HCl, and 0.5 mM EDTA) and heated to 95°C,

followed by gradual cooling to 25°C in a heating block. The resultant double-stranded product (121 bp) was gel purified and subsequently inserted into a *Nhe*I-*Xho*I digested pGL3-promoter plasmid (pGL3p; Promega) to create the pGL3p-5BS FOXM1 luciferase reporter plasmid.

Retroviral Infection Experiments. Retroviral supernatant was produced according to protocol described previously (28), except that the more efficient Phoenix retroviral packaging cells were used. Briefly, Phoenix cells were seeded in 6-cm dishes at 0.5×10^6 cells 24 h before transfection (25 μl Transfast) with retroviral DNA construct (6 μg). After 2 days, the transfected cells were subcultured into 10-cm dishes with the addition of 1.25–2.5 μg/ml puromycin for selection of transfected cells. Once 90% confluent, cells were replaced with normal culture medium without puromycin, and supernatant containing retrovirus was collected once daily two to three times postconfluent. Retroviral supernatant was aliquoted and snap frozen in liquid nitrogen and stored at −80°C until use. Cells to be infected were plated at 10^5 cells/well into 6-well plates 24 h before infection. Each well was preincubated for 10 min in 1 ml of growth medium containing 5 μg/ml Polybrene (hexadimethrine bromide; Sigma) before replacing with 1 ml of retroviral supernatant containing the same concentration of Polybrene. The 6-well plate was then centrifuged ($350 \times g$ at 32°C for 1 h) before retroviral supernatant was replaced with normal growth medium. Transduced cells were incubated for at least 24 h before being used for additional experiments.

Cell Culture. Primary human keratinocytes and telomerase-immortalized N/TERT human keratinocytes (30) were cocultured with γ-irradiated mouse dermal fibroblasts (SWS-3T3) as described previously (31). The immortalised human keratinocyte cell line HaCat and the SCC-derived immortal keratinocyte cell line RTS-3b (32) was maintained in DMEM supplemented with 25% Ham's F12 medium, 10% FCS, and various mitogens (0.4 μg/ml hydrocortisone, 0.1 nM cholera toxin, 5 μg/ml transferrin, 20 pM lyothyronine, 0.18 mM adenine, 5 μg/ml insulin, and 10 ng/ml epidermal growth factor). Other established cell lines [human melanoma A375, human fibrosarcoma HT1080, human embryonic epithelial 293T, Phoenix (293T-derived), and mouse mesenchymal stem-cell C3H10T1/2] were all cultured in DMEM supplemented with 10% FCS. All cells were grown at 37°C in a humidified atmosphere of 5% CO_2/95% air.

Transfection and FOXM1 Reporter Activity Assay. Retrovirally transduced cells were seeded in 6-well plates at 10^5 cells/well 24 h before transfection using Transfast™ Reagent (Promega). For FOXM1 reporter assay, each well was transfected with 20 μl of Transfast containing 1 μg of reporter plasmid pGL3p-5BS and 1 μg of pcDNA3.1-LacZ (Invitrogen, San Diego, CA). Transfected cells were harvested 24 h posttransfection. Cell lysate was vortexed and centrifuged to remove debris, and the supernatant was then assayed for luciferase activity using the Luciferase Assay System (Promega) and β-galactosidase activity using Chlorophenolred-β-D-galactopyranoside (Roche Biochemicals, England, UK) as substrate. Both luminescence and absorbance (595 nm) values were determined using a microtiter platereader (VICTOR^2 Multilabel Counter; Wallac Oy, Turku, Finland). Luminescence data of each sample were normalized for transfection efficiency using the level of β-galactosidase activity in the same sample. All data were subsequently expressed as a percentage of normalized luminescence over controls. Statistical analysis was performed using the GraphPad InStat software (V2.04a; GraphPad Software, San Diego, CA) for Student's *t* test analysis.

Alkaline Phosphatase Assay and Cytochemistry. Retrovirally transduced C3H10T1/2 cells grown in 6-well plates were harvested after 3 days postinfection. Each cell lysate was vortexed and centrifuged to remove debris. AP was assayed in a 96-well plate using a *p*-nitrophenyl phosphate substrate-based AP detection kit (Sigma), according to manufacturer's protocol. Absorbance (at 405 nm) was measured (after 1–2 h 37°C incubation) with a platereader. Protein concentration of each sample was measured (at 595 nm) in parallel using the protein dye Bradford (Sigma) method. AP activity of each sample was normalized for protein concentration and subsequently expressed as a percentage of normalized AP activity over untreated controls. For cytochemical staining of AP, transduced C3H10T1/2 cells grown on glass coverslips placed in 6-well plates were used. AP within cells was detected using a Fast Red Violet naphthol AS-BI phosphate substrate-based AP detection kit (Sigma) according to manufacturer's procedure.

Table 1 *Identification of FOX genes by degenerate PCR and sequence hybridization*

Sample type	Number of clones			
	Total analyzed	FOX clones[a]	FOXM1 clones[b]	Putative FOX clones[c]
Normal human skin	48	28	13	FOXD4(5) FOXD1(2) FOXD2(10)
Cultured primary human keratinocytes	20	10	5	ND[d]
BCCs	48	31	27	FOXD4(3)

[a] Initial number of clones identified to contain a WD sequence.
[b] FOXM1-positive clones were further confirmed by Northern (see Fig. 1*A*) and dot-blot hybridization (data not shown) and by sequencing analysis on nonwinged-helix regions of the gene.
[c] Identity of these putative FOX clones (number of clones) have not been fully characterized.
[d] Not determined.

RESULTS

Identification and Quantification of FOXM1 mRNA in Normal Skin and BCCs. To identify changes in *FOX* gene expression associated with activation of Shh signaling in human skin, we used degenerate PCR to compare pooled RNA from normal skin, cultured primary keratinocytes, and BCC samples (Table 1). More than 58% (28 of 48 clones) of normal skin, 50% (10 of 20) of cultured keratinocytes, and 65% (31 of 48) of BCC clones analyzed matched DNA binding domain of known FOX sequences (including FOXD1, FOXD2, and FOXD4).[6] We did not detect expression of known Shh-activated FOX genes, such as *Foxa2* (HNF-3β; Ref. 15) and *Foxf1* (FREAC-1 or HFH-8; Ref. 17). Among our FOX-positive clones, 46% (13 of 28 normal skin), 50% (5 of 10 keratinocytes) and 87% (27 of 31 BCC) were confirmed to be FOXM1 by PCR, Southern dot-blot hybridization and nucleotide sequencing analyses. FOXM1 has not been previously shown to be expressed in human skin or BCC.

Using Northern blot and densitometric quantification analysis (Fig. 1*A*), we showed that FOXM1 mRNA was dramatically increased in BCCs (FOXM1:β-Actin ratio, 1.89 ± 0.31, $n = 4$) but not in normal human skin (0.06, $n = 2$) and cultured primary human keratinocytes (K°, 0.61 ± 0.02, $n = 2$). FOXM1 mRNA has been shown to be up-regulated in proliferating HeLa cells (18), and hence it was included as a FOXM1-positive control in the Northern blot analysis (Fig. 1*A*). Because Northern analysis is qualitative rather than quantitative, we have resorted to use the LightCycler-based real-time quantitative RT-PCR technique to verify the up-regulation of FOXM1 mRNA in BCCs (Fig. 1*B*). In agreement with the Northern blot analysis, FOXM1 mRNA level in BCC (mean ~6.45 copies of FOXM1 mRNA normalized to 1000 copies of GAPDH mRNA) was significantly higher (~3.4-fold; $P < 0.05$, Student's *t* test) than in normal skin (~1.90 copies). To determine whether FOXM1 expression was specific to BCC and not simply a reflection of increased proliferation, we investigated FOXM1 expression in cutaneous SCCs and proliferating primary keratinocytes. Although FOXM1 mRNA level was slightly elevated in both SCCs (~2.65 copies) and keratinocytes (~3.13 copies) over normal skin (~1.90 copies), these increases were not statistically significant.

Differential Expression of FOXM1 mRNA Isoforms in Skin Tissues and Cultured Cells. Having established that FOXM1 expression is increased in BCCs, we went on to characterize which FOXM1 isoforms are expressed. The genomic structure of FOXM1 gene has been mapped to chromosome 12p13.3 (Genomic Contig; GenBank accession no. NT 009759) consisting of nine exons, two of which (A1 and A2) are alternatively expressed giving rise to three

[6] S-T. Wong and A. G. Quinn, unpublished data.

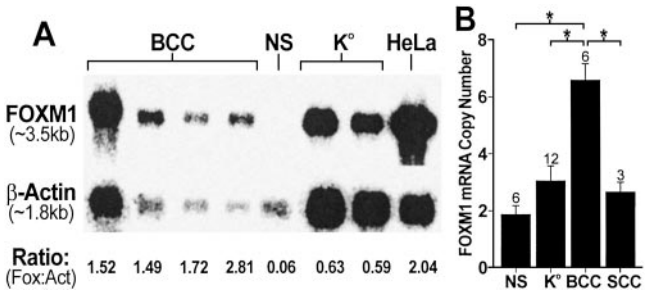

Fig. 1. Quantification of FOXM1 mRNA in human skin samples. *A*, Northern hybridization of FOXM1 and β-actin on skin and cultured cell samples. Each band was densitometrically quantified and subsequently expressed as FOXM1:Actin (*Fox:Act*) ratios. This experiment is a representative of two Northern blots with similar results. *B*, real-time quantitative RT-PCR of FOXM1 mRNA levels (mRNA copy number/1000 copies of GAPDH), using the LightCycler technique, on various human skin samples. Each *bar* represents a mean ± SE of the indicated number of samples tested. The *asterisk* represents data significantly different ($P < 0.05$; Student's *t* test). *NS*, normal nonhairy skin; *K°*, primary cultured human keratinocytes.

differentially expressed mRNA isoforms (Refs. 18 and 33; summarized in Fig. 2*A*). However, little is known about the expression profile of these isoforms in cells or tissues. We have used a semiquantitative RT-PCR method to investigate the relative expression of the three mRNA isoforms (a, b, and c) in various normal and tumor skin tissues and cultured cells using two pairs of primers (FoxF2, R2, F3 and R3; see Figs. 2*B* and 3*A*) designed to amplify across the two alternatively expressed A1 and A2 exons. All three mRNA isoforms were detectable by PCR in all tissues and cell samples studied although with differential pattern of expression between skin tissues and skin-derived cultured cells (Fig. 3, *A* and *B*). We found a predominant expression of FOXM1b isoform in BCCs, SCCs, and normal human skin including hair-bearing skin, whereas FOXM1c isoform was relatively more abundant in cultured cells including primary human keratinocytes (results are summarized in Fig. 3*B*).

FOXM1 Protein Is Abundantly Expressed in BCC but Not in Normal Human Skin or SCC. To further investigate FOXM1 expression in BCCs, we used a previously characterized FOXM1 rabbit polyclonal antibody (18) to immunostain a panel of BCCs from our pathology archives. In keeping with our quantitative RT-PCR results, all seven BCCs examined showed intense extensive positive immunoreactivity throughout the tumor islands (Fig. 4, *A–E*). The antibody detected only a low level of FOXM1 protein in normal interfollicular epidermis or the surrounding stromal cells (Fig. 4*B*). Although FOXM1 has previously been shown to be involved in cell proliferation (19, 22, 34, 35), its immunoreactivity pattern in BCC was distinct from that of proliferation markers such as Ki-67 (Fig. 4*F*) and proliferating cell nuclear antigen (data not shown), which were predominantly localized to the peripheral cell layers of the tumor islands. Within the BCC tumor islands, FOXM1 immunoreactivity was found in both the cytoplasmic and nuclear compartments (Fig. 4, *C–E*). Of

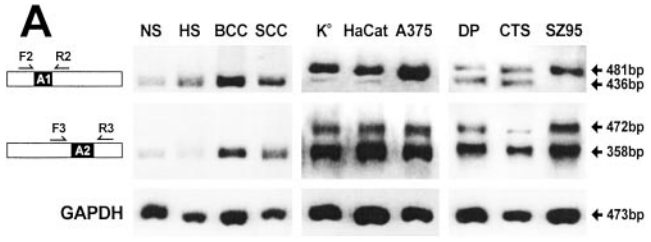

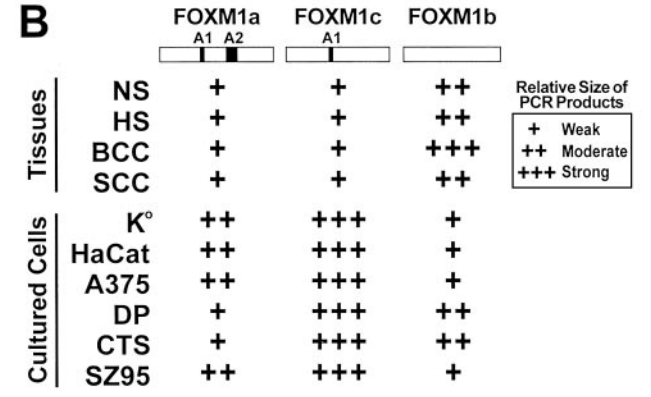

Fig. 3. Relative expression of the three isoforms of FOXM1, determined by semiquantitative RT-PCR by qualitative scoring of the amount of PCR products amplified using two pairs of FOXM1 primers on various skin tissues and skin-derived cultured cells. *A*, representative gel images of PCR products amplified by FoxF2 *versus* R2 (for exon A1) and F3 *versus* R3 (for exon A2) primer pairs, respective positions (not to scale; please refer to Fig. 2*B* for more accurate positions on FOXM1) are indicated on the *left* of the gel images. GAPDH was used as internal control for each sample. These experiments have been repeated three to four times with similar results and are summarized in *B*. *NS*, normal nonhairy skin; *HS*, hairy skin; *K°*, primary cultured keratinocytes; *HaCat*, immortalized keratinocyte line; *A375*, melanoma cell line; *DP*, primary cultured dermal papilla cells from hair follicle; *CTS*, connective tissue sheaths cell line; *SZ95*, sebaceous gland cell line.

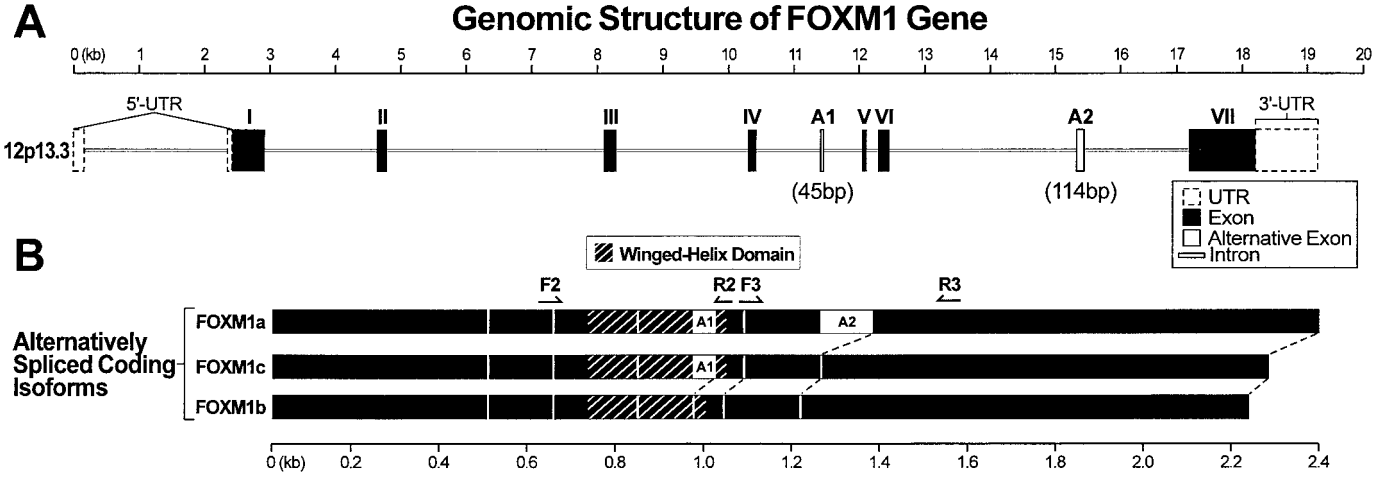

Fig. 2. Genomic structure and coding isoforms of FOXM1 gene. *A*, schematic representation of the genomic structure of FOXM1 gene (18, 33) located in human chromosome 12p13.3 (Genomic Contig; GenBank accession no. NT 009759). The FOXM1 gene consists of seven (I-VII) exons plus two alternatively expressed exons (A1 and A2, 22) generating three alternatively spliced coding isoforms known to date. Exon A2 has been shown to be a transcriptional repressor, whereas exon A1 did not show any apparent transcriptional significance (18).

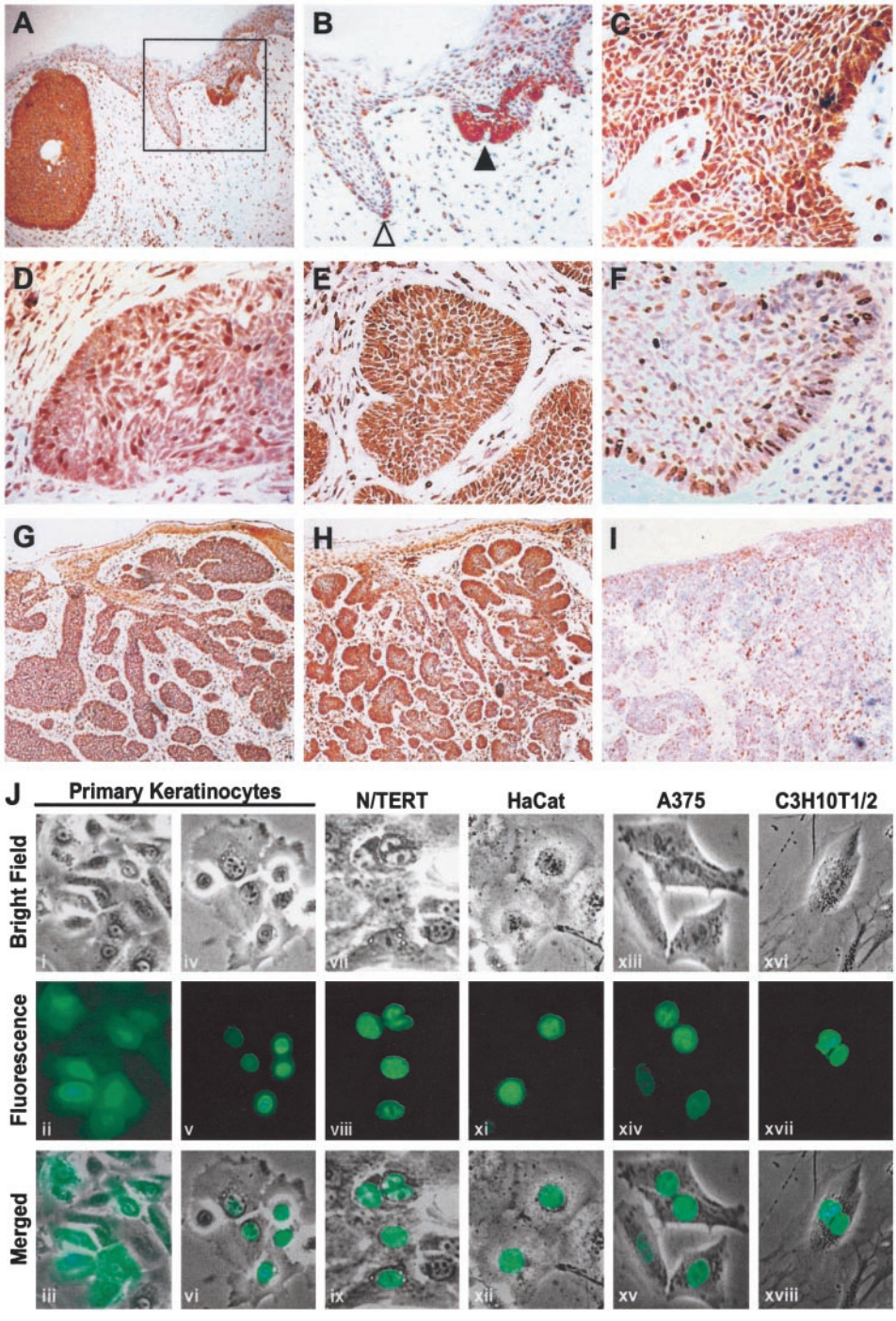

Fig. 4. Pattern of FOXM1 protein expression in BCCs and cultured cells. *A*, immunoreactivity of FOXM1 protein showed a homogenous staining throughout the BCC tumor island but not in an adjacent patch of normal epidermis (*open arrowhead*, see *inset* magnified in *B*) or the adjacent stroma cells. The *filled arrowhead* shows FOXM1 immunoreactivity in a presumed early down-budding (*inset* magnified in *B*) of a BCC tumor. *C–E*, higher magnification (×400) of another three BCC samples showed both cytoplasmic and nuclear immunoreactivity of FOXM1 protein throughout the tumor. *F*, Ki-67 immunoreactive proliferating cells are localized mainly to the peripheral rim of BCC tumor island. *G* and *H*, serial sections of Gli1 (*G*) and FOXM1 (*H*) immunoreactivity within the same BCC sample. *I*, example of FOXM1 immunoreactivity (low/negative staining) in SCC. Similar pattern of FOXM1 immunoreactivity was observed in three other SCC samples (data not shown). *J*, brightfield (*i*, *iv*, *vii*, *x*, *xiii*, *xvi*) and fluorescence (*ii*, *v*, *viii*, *xi*, *xiv*, *xvii*) images of retrovirally transduced primary human keratinocytes, N/TERT, HaCat, A375, and C3H10T1/2 cells expressing either EGFP control (in primary keratinocytes, *i–iii*) or EGFP-FOXM1b fusion protein (*iv–xv*). The fluorescence and brightfield images were merged (*iii*, *vi*, *ix*, *xii*, *xv*, *xviii*) to illustrate the intracellular distribution of the fluorescence proteins.

the seven BCCs studied, three BCCs showed predominantly cytoplasmic staining, two BCC showed predominantly nuclear, and two BCCs showed a mixed pattern of positive FOXM1 immunostaining (see examples in Fig. 4, *A–E*, and data not shown). Serial sections of a BCC tumor sample showed that Gli1 protein (Fig. 4*G*) was coexpressed with FOXM1 (Fig. 4*H*) exclusively within the same BCC tumor. SCCs ($n = 4$) showed negative immunoreactivity for FOXM1 (see an example in Fig. 4*I*).

Intracellular Localization of EGFP-FOXM1b Fusion Protein in Live Cells. To further study the intracellular localization of FOXM1, we expressed an EGFP-FOXM1b fusion protein in a number of skin- and nonskin-related cell types including primary human keratinocytes, the immortalised human keratinocyte cell lines N/TERT and HaCat, the melanoma cell line A375, and the mouse mesenchymal stem cell line C3H10T1/2. Because of the low transfection efficiency on primary keratinocytes using conventional lipid-based transfection method, we have used a highly efficient (>95%), sustained gene expression system using retroviral infection (28). In all these cell types (Fig. 4*J*), as well as a range of other cell types we have tested including an epithelial cell line HeLa, fibrosarcoma cell line HT1080, embryonic epithelial cell line 293T, and an SCC tumor line RTS-3b (data not shown), EGFP-FOXM1 fluorescence was only seen in the nucleus and predominantly in mitotic cells. Cytoplasmic localization of EGFP-FOXM1 fluorescence has not been observed in this study.

FOXM1 Expression is Up-regulated by Gli1. FOXM1b is known to have a role in cell cycle (18, 19, 22, 23, 35, 36), and its

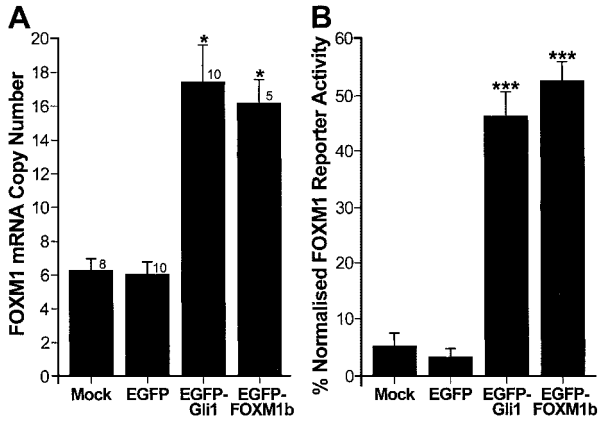

Fig. 5. Induction of FOXM1 mRNA and transcription activity by Gli1 in cultured cells. *A*, retrovirally transduced primary human keratinocytes were harvested 72 h postinfection for quantitative RT-PCR to determine the levels of FOXM1 mRNA (copy number/1000 copies of GAPDH). Each *bar* represents a mean ± SE of the indicated number of samples tested. The *asterisk* indicates that FOXM1 mRNA level is significantly ($P < 0.05$) higher than mock- or EGFP-infected cells. *B*, Luciferase reporter assay for FOXM1 in retrovirally transduced C3H10T1/2 cells. Each *bar* represents a mean ± SE of triplicates. The *three asterisks* indicate that FOXM1 luciferase reporter (pGL3p-5BS) activity is highly significant ($P < 0.001$) over mock- or EGFP-infected cells. This experiment has been repeated at least three times with similar results. Activation of the FOXM1 reporter by Gli1 was also seen in a number of other human cell lines such as HaCat, HeLa, HT1080, and 293T (data not shown).

expression is initiated during G_1 and peaked at G_2/M phase of the cell cycle (19). To determine whether FOXM1 transcription can be regulated independently of the cell cycle by Shh signaling, we have investigated the effect of expressing Gli1, a transcriptional activator that mediates Shh signaling in keratinocytes (12, 13), on FOXM1 gene expression and reporter activity. FOXM1 mRNA level was significantly elevated (~3-fold) in EGFP-Gli1-infected compared with mock- or EGFP-infected keratinocytes (Fig. 5*A*). In agreement, the transcription activity of FOXM1 was significantly activated (~9.4-fold) in retrovirally transduced C3H10T1/2 cells expressing EGFP-Gli1 but not in mock- or EGFP-infected cells (Fig. 5*B*). The EGFP-Gli1-induced levels of FOXM1 mRNA (Fig. 5*A*) and reporter activity (Fig. 5*B*) were comparable with that activated by the positive control EGFP-FOXM1b, indicating that the Gli1-induced FOXM1 mRNA and transcriptional activity reached saturation levels. We have found that Gli1 increased FOXM1 transcriptional activity in all of the human (HaCat, HeLa, HT1080, 293T; data not shown) and murine (C3H10T1/2, Fig. 5*B*) cell lines studied.

Gli1-induced AP Activity Is Independent of FOXM1 in C3H10T1/2 Cells. Activation of an endogenous AP in C3H10T1/2 cells is well characterized and has been widely used as a bioassay for investigating Shh signaling (37–39). We have used this cell-based model system to further investigate the role of FOXM1 in Shh signaling (Fig. 6). As expected, retrovirally transduced C3H10T1/2 cells expressing EGFP-Gli1 dramatically elevated (>18-fold) AP activity over EGFP-expressing cells (Fig. 6*B*). Retinoic acid (1 μM, 24 h pretreatment), a known activator of AP in these cells (40, 41), induced a moderate 10-fold AP activation in mock-infected cells over EGFP-expressing cells. In contrast, AP activity was not activated in EGFP-FOXM1b-expressing cells (Fig. 6*B*).

DISCUSSION

FOX proteins have been shown to play an important role in regulating the expression of genes involved in proliferation and differentiation in many tissues. The functional importance of this family of transcription factors in normal skin biology and their role in skin diseases is unclear because there is a paucity of information on the expression of these genes in the skin. In this study, we have used degenerate PCR to investigate forkhead gene expression and have established that FOXM1, a forkhead gene not previously known to be expressed in human skin, is markedly up-regulated in BCCs, a common keratinocyte-derived Caucasian skin cancer. FOXM1 is known to be ubiquitously expressed in proliferating cells in the mouse embryo and in many cultured cell lines (18–21). In human adult tissue, however, FOXM1 shows a more restricted expression pattern with high expression in the thymus, small intestine, and testis and moderate expression in the ovary (18). We and others have previously established that BCCs are characterized by activated Shh signaling as evidenced by increased expression of the Gli1 transcription factor (11–14). While the increased FOXM1 expression in BCCs could be a reflection of increased cellular proliferation, quantification of FOXM1 mRNA by real-time RT-PCR showed that the marked increase in expression in BCCs was specific to this tumor type and was not seen in cutaneous SCCs that are also hyperproliferative tumors. Increased FOXM1 expression was also not found in proliferating primary human keratinocytes *in vitro*. Furthermore, we did not find expression (by degenerate PCR) of known Shh-activated FOX genes, such as *Foxa2* (HNF-3β; Ref. 15) and *Foxf1* (FREAC-1 or HFH-8; Ref. 17), in neither BCCs nor normal human skin. These findings suggest that the elevation of FOXM1 expression is a characteristic of BCCs and not simply a reflection of increased cell proliferation. This is further supported by our immunostaining studies using a previously characterized FOXM1 antibody (18) that revealed that FOXM1 was uniformly expressed within BCC tumor islands and not confined to peripheral regions of the tumor where proliferating cells (identified using proliferation markers such as PCNA and Ki-67) are predominantly localized. Our observations suggest that FOXM1 expression may under some circumstances be subjected to regulation by noncell cycle-dependent factors because it is unlikely that the extensive expression of FOXM1 within BCC tumor islands is a reflection of cell cycle-related expression alone.

Dissociation between the cell cycle and FOXM1 expression has also been observed during liver regeneration in response to partial hepatectomy where expression of FOXM1 peaks at least 4 h before the onset of DNA replication measured using bromodeoxyuridine incorporation studies (18, 22). In this liver model, FOXM1 immunoreactivity was also found in both the cytoplasmic and nuclear com-

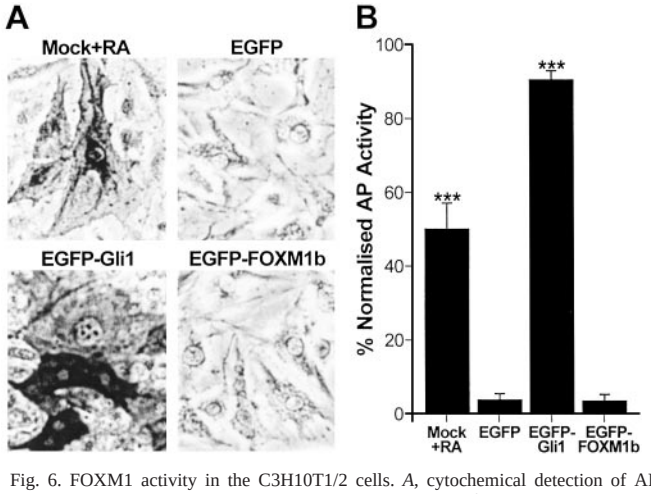

Fig. 6. FOXM1 activity in the C3H10T1/2 cells. *A*, cytochemical detection of AP activity (*dark-colored cells*) within C3H10T1/2 cells. Mock-infected cells treated with retinoic acid (1 μM, 24 h) were used as a positive control for AP induction. *B*, a parallel experiment was performed to quantify the relative levels of AP activity in the corresponding infected cells. Each *bar* represents a mean ± SE of triplicates. The *three asterisks* indicate AP activity is significantly ($P < 0.001$) activated. These experiments have been repeated at least five times with reproducible results.

partments within the hepatocytes. However, nuclear translocation of FOXM1 in the hepatocytes seems to be regulated by mitogenic signaling induced by partial hepatectomy, and this translocation is critical for transcriptional activation of FOXM1 target genes (18, 22, 23). In BCCs the subcellular localization of FOXM1 appears to be more complex with evidence of heterogeneity in tumor samples from different patients. The basis for the heterogeneity and the functional implications of this for the development of this tumor are at present unclear. To further investigate the cellular localization of FOXM1 in keratinocytes, we generated an EGFP-FOXM1b fusion construct. In contrast to the mixed cytoplasmic and nuclear localization seen in keratinocytes within BCC tumor islands *in vivo*, FOXM1 protein was found to be localized predominantly to the nuclei in primary human keratinocytes and a variety of human and murine immortalised cell lines grown in standard culture conditions *in vitro* (Fig. 4*J*). The basis for the differences in the distribution of FOXM1 between expressing cells cultured *in vitro* and expressing cells *in vivo* in BCCs and regenerating liver is not known. The observed differences in the localization of FOXM1 in regenerating hepatocytes between carbon tetrachloride (23) and partial hepatectomy models (18, 22) suggest that while FOXM1 can accelerate hepatocyte regeneration, its subcellular localization regulation and activity is complex and dependent on the nature of the proliferation-inducing stimulus.

A number of FOXM1 isoforms have been identified in previous studies. Genomic structural studies have shown that the human FOXM1 gene maps to chromosome 12p13.3 and consists of nine exons, two of which (A1 and A2) are alternatively expressed (summarized in Fig. 2*B*; Refs. 18 and 33). This gives rise to three different isoforms (a, b, and c). The FOXM1b and c isoforms have been previously shown to be transcriptionally active because of the absence of the inhibitory sequence coded by exon A2. The presence of this exon A2 in isoform FOXM1a renders it transcriptionally inactive (18). Having identified that FOXM1 expression is increased in BCCs, we have shown using RT-PCR that all three known FOXM1 mRNA isoforms were expressed in human skin and cultured cells (Fig. 3), with FOXM1b being the predominant isoform expressed in BCCs.

The identification of FOXM1 up-regulation in BCCs suggests that the *FOXM1* gene may be regulated by Shh signaling. Although FOXM1 has not been previously identified as a downstream target of Shh signaling, other forkhead genes including *Foxa2*, *Foxd2*, and *Foxf1* have been shown to be directly regulated by Shh in some tissues during murine embryonic development (15–17). We have shown that constitutive expression of the transcription factor Gli1, a known target of Shh signaling in mammalian cells, leads to a marked increase in FOXM1 mRNA expression in primary human keratinocytes. Furthermore, we observed coexpression of Gli1 and FOXM1 proteins within the same BCC tumor sample (Fig. 4, *G* and *H*). The increased FOXM1 mRNA expression correlates with an increase in FOXM1 transcriptional activity in Gli1 expressing human and murine cell lines. These observations place FOXM1 downstream of the Gli1 transcription factor and suggest that the regulation of FOXM1 by hedgehog signaling may be an evolutionarily conserved response. Although we have not determined if FOXM1 was a direct transcriptional target of Gli1, a putative Gli-binding element (G<u>C</u>CCACCCA), shows a 1 nucleotide difference (*underlined*) from a previously identified nine nucleotides Gli-binding sequence (G<u>A</u>CCACCCA; Ref. 42), was found at position 2198–2206 of the FOXM1 promoter (GenBank accession no. Y12773). This Gli-binding element is approximately 230 bp upstream of the predicted FOXM1 transcriptional start site (33). Although this putative Gli-binding site is located within a ~300-bp fragment responsible for the cell cycle-specific regulation of FOXM1 expression, it has also been shown that proteins expressed in quiescent and non S-phase cells also interact with this fragment (33), indicating that FOXM1 expression may be regulated by cell cycle-independent proteins.

Shh is known to exhibit context-dependent morphorgenic activities in some tissues (reviewed in Ref. 6). To investigate the morphorgenic aspect of Shh activity that may be mediated by FOXM1 activation, we used the C3H10T1/2 mouse mesenchymal cell line that shows a Shh-dependent activation of an endogenous AP, which can be easily quantified (37–39, 43–45). As expected, overexpression of Gli1 dramatically activated AP activity in these cells. However, overexpression of FOXM1b did not activate AP activity in this cell line, suggesting that FOXM1 is not mediating the morphorgenic signal of Shh via Gli1, which executes the AP-dependent osteoblastic differentiation program in this model system. Shh is also known to act as a mitogen regulating cell proliferation in some tissues (reviewed in Ref. 6). In keratinocytes Shh pathway activation leads to increased epidermal proliferation and the formation of epidermal down-growths that closely resemble BCCs (14), and it has been suggested that this pathway promotes cell cycle progression by inhibiting signals for cell cycle exit or terminal differentiation (46). Similarly, proliferative signaling by Shh is required for the normal expansion of cerebellar granule neurone precursor cells during development, and activation of this pathway is associated with cerebellar tumor development (6, 47, 48).

Although our observations suggest that FOXM1 expression is regulated by a cell-cycle-independent mechanism, studies of FOXM1 transgenic (18, 22) and knockout (35) mice indicate that FOXM1 plays a role in cell proliferation. *In vivo* ectopic expression of FOXM1 in hepatocytes in transgenic mice is associated with accelerated entry into S-phase and mitosis (22). *In vitro* FOXM1 overexpression in cells produces a subtle growth stimulating phenotype that is only detectable following serum deprivation (49). The effects of FOXM1 on the cell cycle are similar to those described in cerebellar granule cultures in response to Shh expression (reviewed in Ref. 6). In this system, Shh promotes DNA synthesis in immature granule cells following serum withdrawal, and this is associated with elevated cyclin D1 levels. The persistent expression of cyclin D1 in this model in response to Shh signaling is similar to the protracted expression of cyclin D1 seen in the transgenic FOXM1-expressing hepatocytes during liver regeneration in response to partial hepatectomy. The similarities between the cell cycle effects seen in these two models is important in the context of our demonstration of a link between Shh signaling and FOXM1 expression for two reasons. First, it raises the possibility that the increase in FOXM1 expression in response to partial hepatectomy could be mediated by activation of Shh signaling. Second, it suggests that the cell cycle effects seen in the cerebellar-granule cell model could be because of an increase in FOXM1 expression. In our preliminary experiment, constitutive overexpression of FOXM1b by retroviral infection of primary keratinocytes did not alter the DNA-content profile (stained by propedium-iodide) of the cell cycle as assayed by fluorescence-activated cell sorting technique.[7] Further work is required to establish if FOXM1 produces a subtle effect on keratinocyte growth *in vitro*. It will also be important in future studies to determine whether the missing link in the partial hepatectomy and cerebellar granule neurone precursor models is the inter-relationship between the Shh signal transduction pathway and the forkhead gene FOXM1, which we have established from our analysis of BCCs in this study.

[7] M-T. Teh and A. G. Quinn, unpublished data.

ACKNOWLEDGMENTS

We are indebted to Dr. David Sugden (King's College London, England, United Kingdom) for technical assistance and permission for using the Light-Cycler system for quantitative RT-PCR, Dr. Robert Costa (University of Illinois at Chicago, Chicago, IL) for providing DNA plasmids and antibody to HFH-11, Dr. Paul Khavari (Stanford University School of Medicine, Stanford, CA) for the retroviral SIN-IP-GFP vector, Dr. Kenneth Kinzler (Johns Hopkins Medical Institutions, Baltimore, MD) for the Gli1 plasmid, and Dr. James Rheinwald (Harvard Institutes of Medicine, Boston, MA) for the N/TERT keratinocytes. We also thank Dr. Alan Storey for advice and critical reading of the manuscript.

REFERENCES

1. Kaufmann, E., and Knochel, W. Five years on the wings of fork head. Mech. Dev., *57:* 3–20, 1996.
2. Kaestner, K. H., Knochel, W., and Martinez, D. E. Unified nomenclature for the winged helix/forkhead transcription factors. Genes Dev., *14:* 142–146, 2000.
3. Lai, E., Prezioso, V. R., Smith, E., Litvin, O., Costa, R. H., and Darnell, J. E., Jr. HNF-3A, a hepatocyte-enriched transcription factor of novel structure is regulated transcriptionally. Genes Dev., *4:* 1427–1436, 1990.
4. Weigel, D., and Jackle, H. The fork head domain: a novel DNA binding motif of eukaryotic transcription factors? Cell, *63:* 455–456, 1990.
5. Ruiz, I. A. A., Sanchez, P., and Dahmane, N. Gli and hedgehog in cancer: tumours, embryos and stem cells. Nat. Rev. Cancer, *2:* 361–372, 2002.
6. Ruiz, I. A. A., Palma, V., and Dahmane, N. Hedgehog-Gli signalling and the growth of the brain. Nat. Rev. Neurosci., *3:* 24–33, 2002.
7. Pathi, S., Pagan-Westphal, S., Baker, D. P., Garber, E. A., Rayhorn, P., Bumcrot, D., Tabin, C. J., Blake Pepinsky, R., and Williams, K. P. Comparative biological responses to human sonic, Indian, and desert hedgehog. Mech. Dev., *106:* 107–117, 2001.
8. Ingham, P. W., and McMahon, A. P. Hedgehog signaling in animal development: paradigms and principles. Genes Dev., *15:* 3059–3087, 2001.
9. Johnson, R. L., Rothman, A. L., Xie, J., Goodrich, L. V., Bare, J. W., Bonifas, J. M., Quinn, A. G., Myers, R. M., Cox, D. R., Epstein, E. H., Jr., and Scott, M. P. Human homolog of patched, a candidate gene for the basal cell nevus syndrome. Science (Washington DC), *272:* 1668–1671, 1996.
10. Xie, J., Murone, M., Luoh, S. M., Ryan, A., Gu, Q., Zhang, C., Bonifas, J. M., Lam, C. W., Hynes, M., Goddard, A., Rosenthal, A., Epstein, E. H., Jr., and de Sauvage, F. J. Activating smoothened mutations in sporadic basal-cell carcinoma. Nature, *391:* 90–92, 1998.
11. Dahmane, N., Lee, J., Robins, P., Heller, P., and Ruiz i Altaba, A. Activation of the transcription factor Gli1 and the sonic hedgehog signalling pathway in skin tumours. Nature, *389:* 876–881, 1997.
12. Ghali, L., Wong, S. T., Green, J., Tidman, N., and Quinn, A. G. Gli1 protein is expressed in basal cell carcinomas, outer root sheath keratinocytes and a subpopulation of mesenchymal cells in normal human skin. J. Invest. Dermatol., *113:* 595–599, 1999.
13. Green, J., Leigh, I. M., Poulsom, R., and Quinn, A. G. Basal cell carcinoma development is associated with induction of the expression of the transcription factor Gli-1. Br. J. Dermatol., *139:* 911–915, 1998.
14. Nilsson, M., Unden, A. B., Krause, D., Malmqwist, U., Raza, K., Zaphiropoulos, P. G., and Toftgard, R. Induction of basal cell carcinomas and trichoepitheliomas in mice overexpressing GLI-1. Proc. Natl. Acad. Sci. USA, *97:* 3438–3443, 2000.
15. Sasaki, H., Hui, C., Nakafuku, M., and Kondoh, H. A binding site for Gli proteins is essential for HNF-3β floor plate enhancer activity in transgenics and can respond to Shh *in vitro*. Development, *124:* 1313–1322, 1997.
16. Wu, S. C., Grindley, J., Winnier, G. E., Hargett, L., and Hogan, B. L. Mouse mesenchyme forkhead 2 (Mf2): expression, DNA binding and induction by sonic hedgehog during somitogenesis. Mech. Dev., *70:* 3–13, 1998.
17. Mahlapuu, M., Enerback, S., and Carlsson, P. Haploinsufficiency of the forkhead gene Foxf1, a target for sonic hedgehog signaling, causes lung and foregut malformations. Development, *128:* 2397–2406, 2001.
18. Ye, H., Kelly, T. F., Samadani, U., Lim, L., Rubio, S., Overdier, D. G., Roebuck, K. A., and Costa, R. H. Hepatocyte nuclear factor 3/fork head homolog 11 is expressed in proliferating epithelial and mesenchymal cells of embryonic and adult tissues. Mol. Cell. Biol., *17:* 1626–1641, 1997.
19. Korver, W., Roose, J., and Clevers, H. The winged-helix transcription factor trident is expressed in cycling cells. Nucleic Acids Res., *25:* 1715–1719, 1997.
20. Yao, K. M., Sha, M., Lu, Z., and Wong, G. G. Molecular analysis of a novel winged helix protein, WIN. Expression pattern, DNA binding property, and alternative splicing within the DNA binding domain. J. Biol. Chem., *272:* 19827–19836, 1997.
21. Chaudhary, J., Mosher, R., Kim, G., and Skinner, M. K. Role of winged helix transcription factor (WIN) in the regulation of Sertoli cell differentiated functions: WIN acts as an early event gene for follicle-stimulating hormone. Endocrinology, *141:* 2758–2766, 2000.
22. Ye, H., Holterman, A. X., Yoo, K. W., Franks, R. R., and Costa, R. H. Premature expression of the winged helix transcription factor HFH-11B in regenerating mouse liver accelerates hepatocyte entry into S phase. Mol. Cell. Biol., *19:* 8570–8580, 1999.
23. Wang, X., Hung, N. J., and Costa, R. H. Earlier expression of the transcription factor HFH-11B diminishes induction of p21(CIP1/WAF1) levels and accelerates mouse hepatocyte entry into S-phase following carbon tetrachloride liver injury. Hepatology, *33:* 1404–1414, 2001.
24. Clevidence, D. E., Overdier, D. G., Tao, W., Qian, X., Pani, L., Lai, E., and Costa, R. H. Identification of nine tissue-specific transcription factors of the hepatocyte nuclear factor 3/forkhead DNA-binding-domain family. Proc. Natl. Acad. Sci. USA, *90:* 3948–3952, 1993.
25. Kaestner, K. H., Lee, K. H., Schlondorff, J., Hiemisch, H., Monaghan, A. P., and Schutz, G. Six members of the mouse forkhead gene family are developmentally regulated. Proc. Natl. Acad. Sci. USA, *90:* 7628–7631, 1993.
26. Ali, R. S., Falconer, A., Ikram, M., Bissett, C. E., Cerio, R., and Quinn, A. G. Expression of the peptide antibiotics human beta defensin-1 and human beta defensin-2 in normal human skin. J. Invest. Dermatol., *117:* 106–111, 2001.
27. Morrison, T. B., Weis, J. J., and Wittwer, C. T. Quantification of low-copy transcripts by continuous SYBR green I monitoring during amplification. Biotechniques, *24:* 954–958, 960, 962, 1998.
28. Deng, H., Lin, Q., and Khavari, P. A. Sustainable cutaneous gene delivery. Nat. Biotechnol., *15:* 1388–1391, 1997.
29. Kinzler, K. W., Bigner, S. H., Bigner, D. D., Trent, J. M., Law, M. L., O'Brien, S. J., Wong, A. J., and Vogelstein, B. Identification of an amplified, highly expressed gene in a human glioma. Science (Washington DC), *236:* 70–73, 1987.
30. Dickson, M. A., Hahn, W. C., Ino, Y., Ronfard, V., Wu, J. Y., Weinberg, R. A., Louis, D. N., Li, F. P., and Rheinwald, J. G. Human keratinocytes that express hTERT and also bypass a p16(INK4a)-enforced mechanism that limits life span become immortal yet retain normal growth and differentiation characteristics. Mol. Cell. Biol., *20:* 1436–1447, 2000.
31. Rheinwald, J. G., and Green, H. Serial cultivation of strains of human epidermal keratinocytes: the formation of keratinizing colonies from single cells. Cell, *6:* 331–343, 1975.
32. Rapp, B., Pawellek, A., Kraetzer, F., Schaefer, M., May, C., Purdie, K., Grassmann, K., and Iftner, T. Cell-type-specific separate regulation of the E6 and E7 promoters of human papillomavirus type 6a by the viral transcription factor E2. J. Virol., *71:* 6956–6966, 1997.
33. Korver, W., Roose, J., Heinen, K., Weghuis, D. O., de Bruijn, D., van Kessel, A. G., and Clevers, H. The human TRIDENT/HFH-11/FKHL16 gene: structure, localization, and promoter characterization. Genomics, *46:* 435–442, 1997.
34. Wang, X., Quail, E., Hung, N. J., Tan, Y., Ye, H., and Costa, R. H. Increased levels of forkhead box M1B transcription factor in transgenic mouse hepatocytes prevent age-related proliferation defects in regenerating liver. Proc. Natl. Acad. Sci. USA, *98:* 11468–11473, 2001.
35. Korver, W., Schilham, M. W., Moerer, P., van den Hoff, M. J., Dam, K., Lamers, W. H., Medema, R. H., and Clevers, H. Uncoupling of S phase and mitosis in cardiomyocytes and hepatocytes lacking the winged-helix transcription factor trident. Curr. Biol., *8:* 1327–1330, 1998.
36. Korver, W., Roose, J., Wilson, A., and Clevers, H. The winged-helix transcription factor trident is expressed in actively dividing lymphocytes. Immunobiology, *198:* 157–161, 1997.
37. Pepinsky, R. B., Rayhorn, P., Day, E. S., Dergay, A., Williams, K. P., Galdes, A., Taylor, F. R., Boriack-Sjodin, P. A., and Garber, E. A. Mapping sonic hedgehog-receptor interactions by steric interference. J. Biol. Chem., *275:* 10995–11001, 2000.
38. Saeki, K., Katsuura, M., Yanagisawa, S., Suzuki, R., Okazaki, M., and Kimura, M. Inactivation of N-terminal signaling domain of sonic hedgehog by forming a disulfide bond. Biochim. Biophys. Acta, *1476:* 219–229, 2000.
39. Williams, K. P., Rayhorn, P., Chi-Rosso, G., Garber, E. A., Strauch, K. L., Horan, G. S., Reilly, J. O., Baker, D. P., Taylor, F. R., Koteliansky, V., and Pepinsky, R. B. Functional antagonists of sonic hedgehog reveal the importance of the N terminus for activity. J. Cell Sci., *112:* 4405–4414, 1999.
40. Reese, D. H., Larsen, R. A., and Hornicek, F. J. Control of alkaline phosphatase activity in C3H10T1/2 cells: role of retinoic acid and cell density. J. Cell. Physiol., *151:* 239–248, 1992.
41. Kennedy, A. R., and Krinsky, N. I. Effects of retinoids, β-carotene, and canthaxanthin on UV- and X-ray-induced transformation of C3H10T1/2 cells *in vitro*. Nutr. Cancer, *22:* 219–232, 1994.
42. Kinzler, K. W., and Vogelstein, B. The GLI gene encodes a nuclear protein which binds specific sequences in the human genome. Mol. Cell. Biol., *10:* 634–642, 1990.
43. Pepinsky, R. B., Zeng, C., Wen, D., Rayhorn, P., Baker, D. P., Williams, K. P., Bixler, S. A., Ambrose, C. M., Garber, E. A., Miatkowski, K., Taylor, F. R., Wang, E. A., and Galdes, A. Identification of a palmitic acid-modified form of human sonic hedgehog. J. Biol. Chem., *273:* 14037–14045, 1998.
44. Spinella-Jaegle, S., Rawadi, G., Kawai, S., Gallea, S., Faucheu, C., Mollat, P., Courtois, B., Bergaud, B., Ramez, V., Blanchet, A. M., Adelmant, G., Baron, R., and Roman-Roman, S. Sonic hedgehog increases the commitment of pluripotent mesenchymal cells into the osteoblastic lineage and abolishes adipocytic differentiation. J. Cell Sci., *114:* 2085–2094, 2001.
45. Nakamura, T., Aikawa, T., Iwamoto-Enomoto, M., Iwamoto, M., Higuchi, Y., Pacifici, M., Kinto, N., Yamaguchi, A., Noji, S., Kurisu, K., Matsuya, T., and Maurizio, P. Induction of osteogenic differentiation by hedgehog proteins. Biochem. Biophys. Res. Commun., *237:* 465–469, 1997.
46. Fan, H., and Khavari, P. A. Sonic hedgehog opposes epithelial cell cycle arrest. J. Cell Biol., *147:* 71–76, 1999.
47. Wechsler-Reya, R. J., and Scott, M. P. Control of neuronal precursor proliferation in the cerebellum by sonic hedgehog. Neuron, *22:* 103–114, 1999.
48. Wechsler-Reya, R., and Scott, M. P. The developmental biology of brain tumors. Annu. Rev. Neurosci., *24:* 385–428, 2001.
49. Leung, T. W., Lin, S. S., Tsang, A. C., Tong, C. S., Ching, J. C., Leung, W. Y., Gimlich, R., Wong, G. G., and Yao, K. M. Over-expression of FoxM1 stimulates cyclin B1 expression. FEBS Lett., *507:* 59–66, 2001.